Systems/Circuits

Coding of Electric Pulse Trains Presented through Cochlear Implants in the Auditory Midbrain of Awake Rabbit: Comparison with Anesthetized Preparations

Yoojin Chung,[1,2] Kenneth E. Hancock,[1,2] Sung-Il Nam,[2,3] and Bertrand Delgutte[1,2,4]

[1]Eaton-Peabody Laboratories, Massachusetts Eye and Ear Infirmary, Boston, Massachusetts 02114, [2]Department of Otology and Laryngology, Harvard Medical School, Boston, Massachusetts 02115, [3]Department of Otolaryngology, School of Medicine, Keimyung University, Daegu, South Korea 700-712, and [4]Research Laboratory of Electronics, Massachusetts Institute of Technology, Cambridge, Massachusetts 02139

Cochlear implant (CI) listeners show limits at high frequencies in tasks involving temporal processing such as rate pitch and interaural time difference discrimination. Similar limits have been observed in neural responses to electric stimulation in animals with CI; however, the upper limit of temporal coding of electric pulse train stimuli in the inferior colliculus (IC) of anesthetized animals is lower than the perceptual limit. We hypothesize that the upper limit of temporal neural coding has been underestimated in previous studies due to the confound of anesthesia. To test this hypothesis, we developed a chronic, awake rabbit preparation for single-unit studies of IC neurons with electric stimulation through CI. Stimuli were periodic trains of biphasic pulses with rates varying from 20 to 1280 pulses per second. We found that IC neurons in awake rabbits showed higher spontaneous activity and greater sustained responses, both excitatory and suppressive, at high pulse rates. Maximum pulse rates that elicited synchronized responses were approximately two times higher in awake rabbits than in earlier studies with anesthetized animals. Here, we demonstrate directly that anesthesia is a major factor underlying these differences by monitoring the responses of single units in one rabbit before and after injection of an ultra-short-acting barbiturate. In general, the physiological rate limits of IC neurons in the awake rabbit are more consistent with the psychophysical limits in human CI subjects compared with limits from anesthetized animals.

Key words: **anesthesia; cochlear implant; inferior colliculus; temporal coding**

Introduction

Although cochlear implants (CIs) restore open-set speech comprehension in a majority of deaf subjects, most CI users still have difficulty with pitch perception, speech reception in noise, and sound localization even with bilateral implantation. These difficulties may stem in part from limitations in temporal processing. A majority of CI users can discriminate the rate of electric pulse trains up to ~300 pulses per second (pps), with a few exceptional subjects showing limits as high as 1000 pps (Townshend et al., 1987; Kong and Carlyon, 2010; Moore and Carlyon, 2010). Responses of auditory neurons to pulse trains delivered through CIs also show an upper limit of temporal coding, but the physiological limits in anesthetized animals are lower than the perceptual limits in human CI users. For the most part, neurons in the inferior colliculus (IC) show sustained and pulse-locked responses to periodic pulse trains only up to 30–300 pps (Snyder et al., 1995; Vollmer et al., 1999, 2005; Middlebrooks and Snyder, 2010; Hancock et al., 2012, 2013). A similar pulse rate limit of 10–200 pps is observed for neural sensitivity to interaural time differences (ITDs) in IC neurons (Smith and Delgutte, 2007; Hancock et al., 2010, 2012), but this limit is lower than that the 250–600 pps limit for perceptual ITD sensitivity in CI listeners (Laback et al., 2007; van Hoesel, 2007). In anesthetized animals, the underlying reason for the limits on temporal coding and ITD sensitivity is that the majority of IC neurons only respond to the onset of pulse trains at rates >100–200 pps. This lack of sustained responses in IC of anesthetized animals is inconsistent with percepts lasting throughout the stimulus even at much higher pulse rates in most CI users, although some subjects experience loudness adaptation (Tang et al., 2006).

We hypothesize that temporal coding, ITD sensitivity, and sustained firing to CI stimulation at high pulse rates may be underestimated due to the effect of anesthesia. Barbiturate anesthesia has been shown to reduce both spontaneous and evoked neural activity in the IC of normal-hearing animals (Bock and Webster, 1974; Kuwada et al., 1989; Torterolo et al., 2002), which is consistent with an enhancement of inhibitory influences. Similar differences between anesthetized and awake conditions have been observed in primary cortex of deaf marmosets and guinea

Received May 16, 2013; revised Oct. 21, 2013; accepted Nov. 13, 2013.

Author contributions: Y.C. and B.D. designed research; Y.C. and S.-I.N. performed research; Y.C. and K.H. analyzed data; Y.C. and B.D. wrote the paper.

This work was supported by the National Institutes of Health (Grants R01 DC005775 and P30 DC005209), Massachusetts Eye and Ear (Curing Kids Fund), and the Hearing Health Foundation (Emerging Research Grant to Y.C.). We thank Connie Miller and Melissa McKinnon for technical assistance and Saori Fukuda, Csilla Haburcakova, Andrew McCall, and Michael Kaplan for advice regarding surgical methods for cochlear implantation in rabbits.

The authors declare no competing financial interests.

Correspondence should be addressed to Yoojin Chung, Eaton-Peabody Laboratory, Massachusetts Eye and Ear Infirmary, Boston, MA 02114. E-mail: yoojin_chung@meei.harvard.edu.

DOI:10.1523/JNEUROSCI.2084-13.2014

 0270-6474/14/340218-14$15.00/0

pigs with CI stimulation (Johnson et al., 2011; Kirby and Middlebrooks, 2012). A degradation of temporal coding by anesthesia has been reported in the IC (Tollin et al., 2004; Song et al., 2011) and auditory cortex (Ter-Mikaelian et al., 2007) of normal-hearing animals.

We developed an awake rabbit model of CIs for single-unit recording from the IC to eliminate the confound of anesthesia. Although awake preparations are increasingly common in single-unit studies of normal-hearing animals, they have not yet been used to study responses of subcortical auditory neurons to CI stimulation in deaf animals. Our results show higher pulse rate limits of temporal coding in the awake rabbit compared with earlier results from anesthetized preparations. We also found unsynchronized, sustained responses at high pulse rates that are rarely observed in the IC of anesthetized animals with CI stimulation. We demonstrate that these differences are largely due to the effect of anesthesia by monitoring the responses of single units in one rabbit before and after injection of an ultra-short-acting barbiturate.

Materials and Methods

Animals

We measured responses of single units in the IC of awake rabbits to electric stimulation presented through CIs. Experiments were performed on four female Dutch-belted rabbits, two of which received unilateral cochlear implantation in the right ear and the other two bilateral cochlear implantations. All procedures were approved by the animal care and use committees of both Massachusetts Eye and Ear and the Massachusetts Institute of Technology. A preliminary report of some of these findings has been published previously (Chung et al., 2013).

Surgical procedures

Methods for recording from single units in the IC of awake rabbits were as described in previous reports with normal-hearing animals (Devore and Delgutte, 2010; Day et al., 2012). Methods for chronic cochlear implantation in adult rabbits were newly developed. Anesthesia for all survival surgeries was induced with xylazine (5–6 mg/kg, s.c.) and ketamine (35–44 mg/kg, i.m.). For prolonged surgeries such as cochlear implantation, a surgical level of anesthesia was maintained by isoflurane mixed with oxygen (2.5%) and delivered via a facemask (0.8 l/min).

Each rabbit underwent three surgical procedures separated by recovery and training periods: a first one to affix a headpost and stainless steel cylinder to the skull, a second one to implant intracochlear electrode arrays, and a third one to perform a craniotomy for accessing the IC. In the first surgery, a stainless steel cylinder and brass head bar were affixed to the skull using stainless steel screws and dental acrylic (Jet Denture Repair; Lang Dental). After the rabbit was fully recovered, surgery for cochlear implantation was performed. A postauricular incision was made to access the tympanic bulla and then part of the bulla was drilled to expose the round window. An eight-contact ring-type electrode array (Z60274; Cochlear Ltd) was inserted into the cochlea through the round window. Before inserting the electrode array, 5–10 μl of distilled water was injected into the cochlea through the round window to deafen the ear by causing hypotonic stress to the organ of Corti (Ebert et al., 2004). The round window was sealed with soft tissue harvested from nearby muscle and secured with dental cement (Durelon; 3M). The percutaneous connector terminating the lead wire of the electrode array was secured to the side of the headpost with dental acrylic. The superficial muscles and the skin incision were closed with sutures that were removed 10–14 d after the operation. Success of cochlear implantation was verified immediately after surgery by measuring the electrically evoked auditory brainstem response (EABR) to biphasic current pulses delivered between the most apical and the most basal electrodes in the intracochlear array. EABR thresholds were usually in the range of −16 to −12 dB re 1 mA. The ABR to 100 μs acoustic clicks at 100 dB peak SPL was also measured to verify the effectiveness of deafening in the implanted ears. No attempt was made to deafen the unimplanted left ear in the two unilaterally implanted rabbits.

After an ~1 week recovery from cochlear implantation surgery, rabbits were habituated to the experimental setup until they could sit quietly for 2–3 h with the head attached by the headpost while receiving electric stimulation through the cochlear implant. After habituation, the animals underwent a third aseptic procedure to make a small (~2 mm diameter) craniotomy 10.5 mm posterior and 3 mm lateral to bregma. In the two unilaterally implanted rabbits, the craniotomy was made contralateral to the implanted right ear. The exposed area was covered with a topical antibiotic (Bacitracin) and sealed with dental impression material (Reprosil). Single-unit recording sessions started after 2–3 d of recovery and lasted until 26–431 d after implantation. Rabbits were monitored on a closed-circuit video system throughout the recording sessions and only received auditory stimulation through their cochlear implant during the recording sessions.

Electrophysiological methods

Stimuli. The main stimuli were 300 ms periodic trains of biphasic pulses (50 μs/phase) presented every 600 ms. Pulse trains were generated using 16-bit D/A converters (PXI-6221; National Instruments) and delivered to each cochlear implant through a pair of custom-built, high-bandwidth, isolated current sources. Stimulation was between the most apical and most basal intracochlear electrodes. This wide bipolar electrode configuration stimulates auditory nerve fibers over the entire length of the tonotopic axis while reducing stimulus artifact relative to monopolar stimulation (Litvak et al., 2001). Stimuli were presented diotically in the bilaterally implanted rabbits and monaurally to the ear contralateral to the recorded IC in the unilaterally implanted rabbits.

The stimulus used for searching for single units in bilaterally implanted rabbits was a sequence of three biphasic pulses presented alternately to both ears (diotically), the left ear, and the right ear. The interval between consecutive pulses in the triplet was 100 ms and the silent interval between triplets was 200 ms. In unilaterally implanted rabbits, the search stimulus was a pair of pulses separated by 100 ms with a 300 ms silent interval between pairs.

Single unit recordings. Single units were isolated using epoxy-insulated tungsten electrodes (A-M Systems) advanced with a remote-controlled microdrive. The electrode was advanced in a dorsoventral direction through the occipital cortex up to the IC, which was identified by background entrainment to the search stimuli. Signals from the recording electrode were preamplified (Axoprobe 1A; Molecular Devices), band-pass filtered (1–3 kHz), and sampled at 100 kHz using a high-speed, 12-bit A/D converter (PXI-6123; National Instruments). The stimulus artifact was removed by gating out a short interval (0.3–0.5 ms) after each stimulus pulse. Spike times were detected by software triggering on level crossings. Only well isolated single units were studied, as assessed by the stability of spike waveforms and amplitudes, which were always at least three times above the noise floor and clearly distinct from the local field potential. Representative spike waveforms recorded from IC neurons are shown in Figure 1, *A–C*, for pulse-train stimulation. These examples include a range of spike quality, from excellent (Fig. 1*C*) to cases that are clearly single units but include a small fraction (<1%) of false triggers (Fig. 1*A*,*B*).

When a single unit was isolated, the threshold for a single biphasic pulse was determined by measuring responses to the search stimulus from just below threshold to at least 2 dB above threshold in 1 or 2 dB steps. Then responses to 300 ms pulse trains were measured for pulse rates ranging from 20 to 1280 pps in half-octave steps. Pulse rates were presented in random order and each rate was repeated 12–20 times. Pulse trains were presented at 2–4 dB above the single-pulse threshold.

Histological processing. In the last recording session from one unilaterally implanted rabbit, electrolytic lesions were made to mark the borders of the region showing activity evoked by CI stimulation while the animal was under deep anesthesia (xylazine 6 mg/kg, s.c., and ketamine 44 mg/kg, i.m.). The rabbit was then perfused intracardially using a solution of 1.5% paraformaldehyde and 2.5% gluteraldehyde in phosphate buffer. The brain was immersed in fixative for 24 h and then transferred to 25% sucrose solution for several days. Coronal sections (80 μm) were cut with

a freezing microtome and mounted on subbed slides. Borders of IC regions were identified by staining cell bodies with azure-thionin. All identified lesions were located within the central nucleus.

Injection of ultra-shorting-acting barbiturate

To assess the effect of anesthesia in individual neurons directly, a catheter was surgically inserted into the right jugular vein of one unilaterally implanted rabbit to allow the administration of an ultra-short-acting barbiturate while recording from single units (Kuwada et al., 1989). A median ventral neck incision was made to expose the bifurcation of the right jugular vein into the anterior and posterior facial veins. A silicon catheter (2 Fr/outer diameter 0.67 mm, 20 cm) filled with diluted heparin (10 U/ml) was inserted at ~6 cm, approximately to the level of the superior vena cava, into the posterior facial vein just above the bifurcation point. The catheter was secured to the vein with ligatures and led subdermally to an injection port on the nape of the neck. The catheter was flushed with diluted heparin (10 U/ml) every day and after each use to keep it patent (Kaplan and Timmons, 1979; Kuwada et al., 1989).

In recording sessions from this rabbit, the responses of a single unit to pulse trains were first characterized in the awake condition as a function of pulse rate using 12 repetitions as described above. Following this characterization, 5 mg/kg methohexital sodium (Brevital) was injected through the intravenous catheter over 10 s. The unit responses to pulse train stimuli were then monitored for 10–30 min after the injection, yielding 80–240 repetitions of responses to 12 different pulse rates. Up to two injections separated by at least 30 min were given over a 2 h recording session. A total of 13 injections were made in this rabbit while successfully maintaining contact with a single unit.

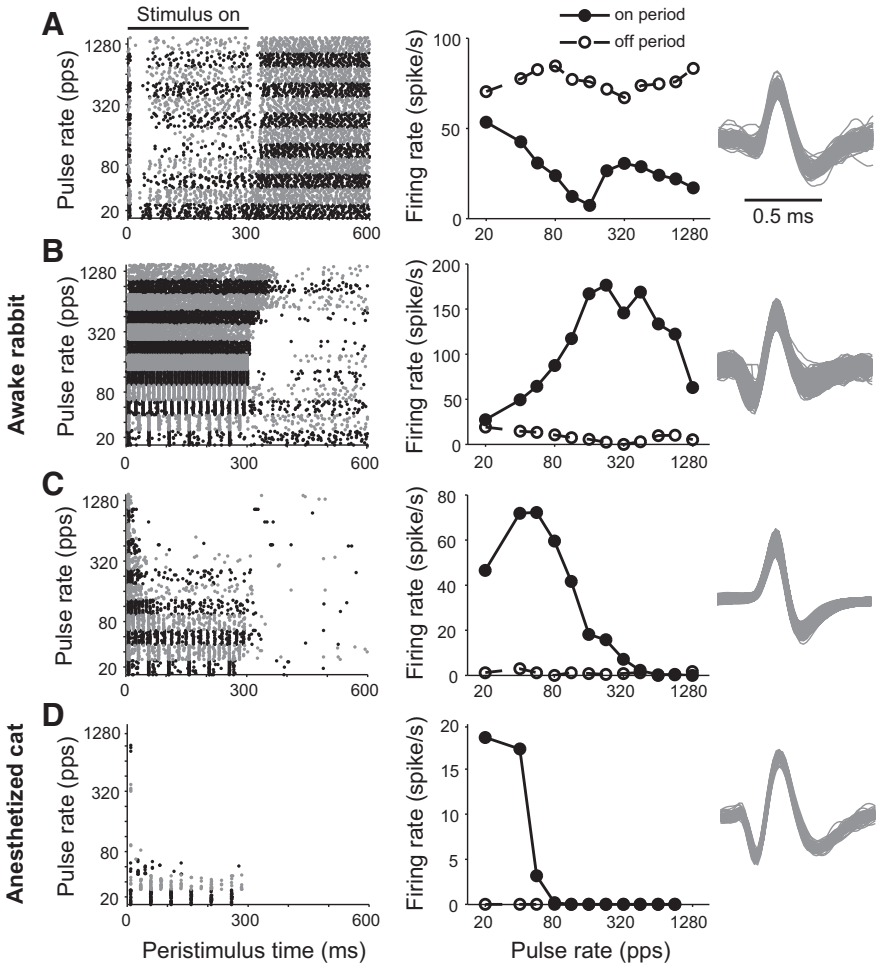

Figure 1. Temporal response pattern (left), average firing rates (middle), and spike waveforms (right) in response to trains of biphasic pulses of different rates for three example IC neurons in awake rabbit (***A–C***) and one neuron from anesthetized cat (***D***). Left: Dot-rasters in which each dot represents a spike and alternating shades of gray distinguish blocks of stimulus trials at different pulse rates. Middle: Mean firing rates during the on period (excluding the first ~30 ms after stimulus onset) and off period (excluding the first 100 ms after stimulus offset) versus pulse rate. Right: Superimposed spike waveforms from each neuron (145, 314, 227, and 95 spikes, respectively).

Single unit recordings from anesthetized cats

Because direct data on the effects of anesthesia were only available from a small number of neurons, we reanalyzed data from the IC of anesthetized cats that have been described in part previously (Hancock et al., 2010, 2012, 2013) to allow quantitative comparison with the awake rabbit data at the population level. These data came from six adult cats that were deafened with ototoxic drugs and received cochlear implants bilaterally at the beginning of the neurophysiological experiment.

In the first of two procedures, adult cats were deafened by injection of kanamycin (300 mg/kg, s.c.) followed after 30 min by ethacrynic acid (25 mg/kg, i.v.; Xu et al., 1993) while under ketamine anesthesia (33 mg/kg, i.m.). The effectiveness of deafening was verified by the absence of ABR response to 100 μs acoustic clicks up to 100 dB peak SPL (Hancock et al., 2010). The neurophysiological experiment took place either 1–2 weeks ($n = 3$) or 6 months ($n = 3$) after deafening. Cats were anesthetized with a combination of urethane (300 mg/kg, i.p.) and either diallyl barbituric acid (75 mg/kg, i.p.) or sodium pentobarbital (37 mg/kg, i.p.). The lateral and dorsal aspects of the skull were exposed. Tympanic bullae were opened bilaterally to allow access to the round window. A small cochleostomy was made and eight-contact electrode arrays (Z60274; Cochlear Ltd) were inserted bilaterally. An opening was made in the skull and the dorsal surface of the IC was exposed by aspirating the overlying cerebral cortex and removing part of the bony tentorium.

Aside from the use of anesthesia in cat, all stimulation protocols, recording procedures, and methods for data analysis were essentially the same in cat and in rabbit except for minor differences. Single-unit recordings in cat were made using 16-site multichannel electrodes (Neuronexus) advanced dorsally to ventrally into the exposed IC. Signals were preamplified (RA16; TDT) and then filtered (300–3000 Hz) and amplified using a digital signal processor (Medusa; TDT). The recording was typically made differentially between adjacent electrodes in the array to minimize the amplitudes of stimulus artifacts and local field potentials. Criteria for defining single units were the same as in rabbit. Figure 1*D* shows spike waveforms from an example neuron in anesthetized cat.

Data analysis

Spontaneous activity. In some units, spontaneous activity was recorded for 30 s without any stimulation. In cases when the spontaneous activity was not measured directly, we used responses to the search stimulus to estimate the spontaneous firing rate. Specifically, we counted the spikes occurring at subthreshold levels when available. If too few subthreshold responses were available, spikes were counted over the last 100 ms of the 200–300 ms silent interval between consecutive search stimuli and averaged over all tested levels.

Dependence of average firing rate on pulse rate. To compute the "sustained" firing rate in response to the 300 ms pulse trains, the onset response was removed by excluding the smallest integer number of

stimulus periods having a total duration of at least 30 ms. The firing rate was averaged over the remaining stimulus duration with the onset window excluded. In awake rabbits, both background activity and rebound responses after stimulus offset were observed frequently. To minimize the effect of rebound responses, the spike rate during the off period was calculated over a 200 ms window extending from 100 ms after stimulus offset to the onset of the next stimulus.

To test for stimulus-driven activity (excitatory or suppressive) for each pulse rate, we used receiver operating characteristic analysis to compare the sustained firing rates during the on and off periods on a trial-by-trial basis. A response was considered to be significantly excitatory if the firing rate during the on period exceeded the rate during the subsequent off period in at least 75% of stimulus trials. Conversely, the response was considered to be suppressive if the rate during the off period exceeded the rate during the on period in at least 75% of stimulus trials.

A spike will be undetected if the portion of its waveform exceeding the user-set threshold occurs entirely during the 0.3–0.5 ms stimulus artifact gating window. These missed spikes result in firing rates being underestimated, especially for high pulse rates, when the gating window covers a substantial fraction of the stimulus period. This underestimation of firing rates during the on period could lead to responses being incorrectly identified as suppressive when they are compared with the off period response, in which there is no artifact gating. To avoid this problem, all apparently suppressive responses were corrected by recomputing the on period firing rate using a stimulus duration excluding the gating windows. This correction assumes that spikes are equally likely to occur within and outside of the gating windows. No correction was applied to putatively excitatory responses to avoid overestimating the firing rate in case this assumption does not hold. This method ensures a conservative identification of both excitatory and suppressive responses.

Cluster analysis of on and off period responses. We observed considerable variability between neurons in both the dependence of responses on pulse rate and on the relative magnitudes of responses during and after the stimulus. To characterize this variability objectively, we used *k*-means clustering (MATLAB; MathWorks) to categorize neurons based on the joint pulse-rate dependence of on and off responses. For each neuron, the sustained firing rate versus pulse rate curves during the on and off periods were concatenated into a single vector and then normalized by the maximum value over the entire vector. The clustering algorithm iteratively partitions the set of vectors (one for each neuron) into a prespecified number of clusters to minimize the sum of the Euclidean distances of each vector to the cluster centroid. The number of clusters was chosen by monitoring the summed Euclidean distance between neural responses and the cluster centroid as a function of the number of clusters.

Pulse-locked responses. Two different methods were used to characterize the synchronization of spikes to the stimulus pulses and to determine an upper rate limit of pulse locking for each unit, a method based on cross-correlation between stimulus and response (Hancock et al., 2013) and a more standard method based on vector strength, a.k.a. synchronization index (Vollmer et al., 2005; Middlebrooks and Snyder, 2010). The two methods differ in that the cross-correlation method requires spikes to occur within a relatively narrow latency range after each pulse to be considered pulse locked, whereas all spikes contribute to the vector strength regardless of when they occur over the stimulus period.

The following description of the cross-correlation analysis supersedes that in our earlier report (Hancock et al., 2013), which was oversimplified. For each pulse rate, the stimulus pulse train was cross-correlated with the spike train (excluding the onset response) and a histogram constructed using a 0.1 ms bin width. When properly normalized, this cross-correlogram represents the mean instantaneous firing rate after each stimulus pulse. A perfectly pulse-locked response would yield a single peak at the spike latency in the cross-correlogram. To assess the statistical significance of cross-correlogram peaks, we computed cross-correlograms for random spike trains containing the same number of spikes as the data, but uniformly distributed over the sustained response window excluding the artifact gating windows. This computation was repeated for 5000 random spike trains and a confidence bound was defined as the 99.5th percentile ($p = 0.005$) of these synthetic cross-correlograms (Fig. 3*A*,*B*, gray shading). A correlogram peak was regarded as significant when the average of two consecutive bins exceeded the confidence bound. The height of the largest peak in the cross-correlogram (after averaging consecutive bins) relative to the 99.5% confidence bound was used as a measure of the strength of pulse locking. The pulse-locking limit was computed by interpolating to find the pulse rate where the peak height intercepted the confidence bound (Fig. 3*C*,*D*). Spike latency was defined as the latency of the highest significant peak in the cross-correlogram. The latencies were averaged over all pulse rates up to 80 pps to get a single latency for each unit.

The cross-correlograms were also used to separate pulse-locked spikes from unsynchronized spikes and to define a pulse-locked firing rate for each pulse rate. For this purpose, we used the area of each significant cross-correlogram peak lying above the average firing rate (Fig. 3*A*,*B*, white filled areas). Some units fired at multiple latencies within an interpulse interval and therefore showed multiple peaks in their cross-correlogram. In such cases, the peak areas were summed over all significant peaks. The summed peak areas were converted to units of firing rate (spikes/s) for comparison with the overall firing rate.

Vector strength was computed for each unit and each pulse rate using the method of Goldberg and Brown (1969). The statistical significance of the vector strength is usually assessed by the Rayleigh test (Yin and Kuwada, 1983), which assumes a uniform distribution of spikes over the stimulus period under the null hypothesis. This test is not applicable to our data because spikes occurring during the stimulus artifact gating window are not detected, resulting in a nonuniform distribution even when spikes are not synchronized to the pulse train. We therefore used the same 5000 random spike trains as for the cross-correlation analysis to calculate a 99.5th confidence bound for vector strength and assessed statistical significance by comparing the measured vector strength to the bound for each pulse rate. This test would be equivalent to the Rayleigh test (with $p < 0.005$) if there were no artifact gating. A pulse-locking limit was determined for each unit by interpolating to find the pulse rate where the vector strength intercepted the confidence bound (Fig. 3*E*,*F*). The confidence bounds for vector strength (Fig. 3*E*,*F*, dashed lines) increase with pulse rate because the artifact gating window occupies an increasing fraction of the stimulus period.

Results

We recorded from 136 single units in the IC of awake rabbit, 94 units from two unilaterally deafened and implanted rabbits and 42 from two bilaterally deafened and implanted rabbits. The single-unit recordings from unilaterally implanted rabbits were made 29–431 d after implantation, whereas the recordings from bilaterally implanted rabbits were made 26–172 d after implantation. Unless otherwise noted, responses to contralateral stimulation in unilaterally implanted rabbits and to diotic stimulation in bilaterally implanted rabbits were combined because the patterns of response were similar.

Dependence of firing rates on pulse rate

Responses to periodic electric pulse trains were measured as a function of pulse rate in all neurons. We observed wide variability in both the pulse-rate dependence of responses and the relationship between responses during the on and off periods. Responses of three example units from awake rabbit and one unit from anesthetized cat are shown in Figure 1. The first neuron from awake rabbit (Fig. 1*A*) illustrates the suppressive responses (except for an onset response) that are commonly observed in this preparation. A very high level of background activity (~70 spikes/s) is observed during the interstimulus period; this activity is suppressed during presentation of the pulse train, with the greatest suppression occurring at 160 pps. In contrast, the second neuron from awake rabbit (Fig. 1*B*) shows excitatory responses for all pulse rates and lower background activity. The neuron fires approximately one spike per pulse up to 160 pps in a pulse-locked manner, as indicated by periodic patterns in the dot raster. Pulse-

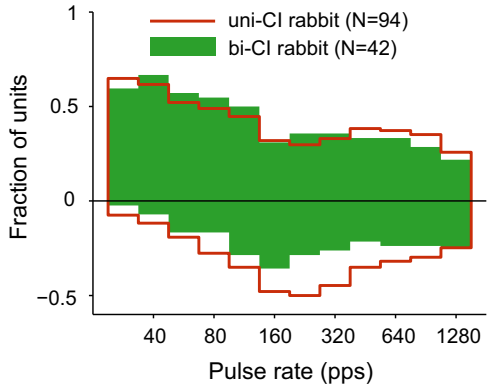

Figure 2. Fraction of IC units showing excitatory (positive ordinates) and suppressive (negative ordinates) responses to pulse-train stimulation as a function of pulse rate in unilaterally implanted and bilaterally implanted rabbits.

locked firing at low rates transitions to unsynchronized firing at high rates, and sustained responses are observed up to the highest rate tested (1280 pps). The background activity is suppressed after each stimulus, especially at intermediate pulse rates that evoke the largest sustained response. Although the types of responses illustrated in Figure 1, *A* and *B*, are primarily observed in awake rabbit, responses such as those of the rabbit neuron in Figure 1*C* are observed in both awake and anesthetized preparations (Hancock et al., 2012). This neuron fires approximately two spikes per pulse at 20 pps; firing efficiency starts to decrease from 56 pps up and only a response to the first pulse is observed for rates >320 pps, resulting in a "band-pass" pattern for the sustained response. Finally, the pattern illustrated by the neuron from anesthetized cat in Figure 1*D* is rarely observed in awake rabbit. This neuron fires one spike per pulse at 20 pps, but firing efficiency starts to decrease from 40 pps up and there is only a response to the first pulse for rates >80 pps. The lack of background activity during the interstimulus period in Figure 1*D* contrasts with the strong spiking in neurons from awake rabbit in Figure 1, *A* and *B*.

The firing rates during the on period (excluding the onset response) and the off period (excluding the first 100 ms) were compared for each pulse rate to determine whether the pulse train elicited a significant excitatory or suppressive response (see Materials and Methods). Figure 2 shows the fraction of units that showed significant excitatory and suppressive responses as a function of pulse rate for all neurons from awake rabbit. The data are shown separately for unilaterally and bilaterally implanted animals. The bars on the positive side represent the fraction of units that show significant excitatory activity; those on the negative side represent suppressive activity.

In both unilaterally and bilaterally implanted animals, excitatory responses dominate for pulse rates up to 80 pps, with >50% of units showing excitatory responses and <30% showing suppressive responses. The fraction of excitatory responses decreases with increasing pulse rate at low rates, with a concomitant increase in the fraction of suppressive responses. For pulse rates of 160 pps and above, excitatory and suppressive responses are approximately balanced, with 25–40% of the units showing excitatory responses and 25–50% showing suppressive responses. Suppressive responses are more frequently observed in unilaterally implanted animals than in bilaterally implanted animals >160 pps. A two-way ANOVA on the arc-sine-transformed fraction of suppressive responses showed significant effects of both pulse rate and unilateral versus bilateral implantation ($p < 0.001$ for both). A parallel ANOVA for excitatory responses showed significant effects of pulse rate ($p < 0.001$), but no effect of type of implantation ($p = 0.76$).

The greater incidence of suppressive responses in unilaterally implanted animals might reflect increased spontaneous activity compared with bilaterally implanted animals. However, there were no significant differences in the distributions of either spontaneous firing rates (Kolmogorov–Smirnov, $p = 0.18$) or firing rates during the interstimulus off period (Kolmogorov–Smirnov, $p = 0.41$) between unilaterally and bilaterally implanted rabbits.

Pulse-locked responses and response latency

The degree of synchronization ("pulse-locking") between neural spikes and stimulus pulses was assessed using two complementary methods: one based on cross-correlation between spike trains and stimulus pulse trains (Hancock et al., 2013) and the traditional method based on vector strength (Vollmer et al., 2005; Middlebrooks and Snyder, 2010). The cross-correlation method should provide a more stringent criterion for pulse locking because it requires spikes to occur within a restricted range of latencies after each stimulus pulse, whereas the vector strength method counts all spikes regardless of their temporal position over the stimulus period (Hancock et al., 2013). Figure 3*A*,*B* shows example cross-correlograms for the same rabbit IC neurons as in Figure 1, *C* and *B*, respectively. Robust pulse locking was evoked by low-rate pulse trains in both neurons, as shown by prominent peaks at a latency of ~6 ms in the cross-correlograms. The peak amplitude dropped markedly (>112 pps) in the first neuron (Fig. 3*A*) and firing was minimal (>224 pps). In contrast, pulse-locked spikes were observed up to 320 pps in the other neuron (Fig. 3*B*). The multiple cross-correlogram peaks for pulse rates between 80 and 320 pps reflect the periodicity of the pulse train stimulus. Above 320 pps, no cross-correlogram peak exceeds the 99.5% confidence bound for a random spike train (gray shading), meaning that the responses are unsynchronized to the stimulus pulses.

For each neuron, the pulse-locking limit was defined as the highest pulse rate where a significant peak was observed in the cross-correlogram (see Materials and Methods). Figure 3, *C* and *D*, shows the normalized height of the correlation peaks relative to the 99.5% confidence bound for random spike trains as a function of pulse rate. The pulse-locking limit is the rate where the normalized peak height just falls below 1, meaning the correlation peak no longer exceeds the confidence bound. The pulse-locking limits were 156 and 356 pps for the two example neurons. In comparison, Figure 3, *E* and *F*, show the vector strength and its 99.5% confidence bound for a random spike train as a function of pulse rate for these two neurons. Pulse-locking limits determined by the vector strength method were 220 and 312 pps.

The area of the significant cross-correlogram peaks lying above the average firing rate (Fig. 3*A*,*B*, white filled area) was used to define a "pulse-locked firing rate" that was compared with the overall sustained firing rate during the on period (comprising both pulse-locked and unsynchronized spikes). Pulse-locked firing rates are shown as a function of pulse rate and compared with overall firing rates for the two example neurons in Figure 3, *G* and *H*. In the first neuron, the overall and pulse-locked firing rates approximately parallel each other, which is consistent with the decrease in firing rates near the pulse-locking limit (Figs. 1*C*, 3*A*). In contrast, in the other neuron, the pulse-locked firing rate falls sharply above 224 pps, whereas the overall firing rate remains substantial up to the highest rate tested, re-

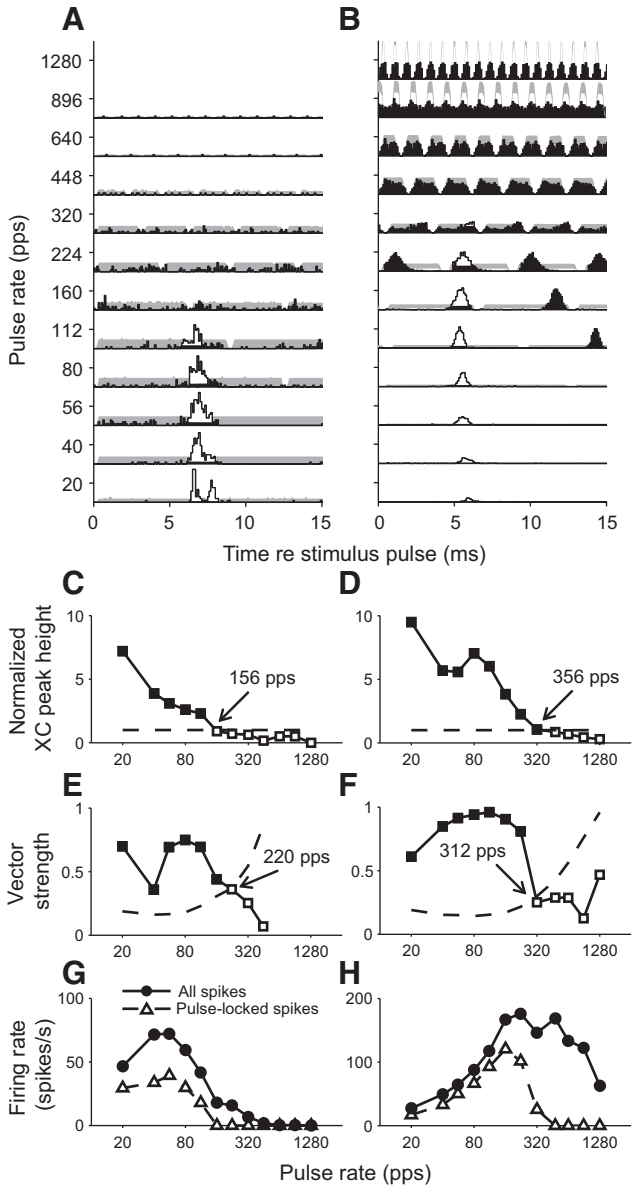

Figure 3. ***A, B***, Cross-correlograms between stimulus pulse trains and neural spike trains for the same two neurons as in Figure 1, *C* and *B*, respectively. Each trace shows the cross-correlogram for one pulse rate. Gray shading indicates the 99.5% upper confidence bound for a random spike train; correlation peaks exceeding the confidence bound are filled in white. ***C, D***, Normalized height of the main correlogram peak as a function of pulse rate. The peaks are normalized to the 99.5% confidence bound (dashed line). Filled marker indicates that the peak height exceeds the confidence bound. The pulse-locking limit is defined as the rate where the peak height intercepts the 99.5% upper confidence bound. ***E, F***, Vector strength and 99.5% upper confidence bound for a random spike train as a function of pulse rate. The limit is defined as the rate where the vector strength intercepts the 99.5% upper confidence bound. ***G, H***, Comparison of firing rates computed using all spike to firing rates computed using only pulse-locked spikes.

flecting the change from a pulse-locked firing pattern at low rates to unsynchronized firing at high rates (Figs. 1*B*, 3*B*).

The distributions of pulse-locking limits obtained by both methods in awake rabbit are compared in Figure 4*A* and Table 1 (the cat data also included in Table 1 will be discussed later). The main difference between the two methods is the much higher fraction of neurons that did not pulse lock at any rate using the cross-correlation method (29%) compared with using vector strength (6%), which is consistent with the idea that the cross-correlation method provides a more stringent criterion for pulse locking. Differences between the two methods were minimal when only pulse-locking units were considered and the median pulse-locking limits were similar (148 pps for cross-correlation vs 158 pps for vector strength). Neither the differences in the shapes of the distributions (as assessed by the Kolomogorov–Smirnov test), nor the difference in median pulse-locking limits (Wilcoxon rank-sum test) reached statistical significance (Table 1).

Using the cross-correlation method, there was no significant difference in median pulse-locking limits for contralateral stimulation in unilaterally implanted rabbits compared with diotic stimulation in bilaterally implanted rabbits (Wilcoxon rank-sum test, $p = 0.11$). In addition, no significant difference in median pulse-locking limits between contralateral and bilateral stimulation was observed among 20 neurons from bilaterally implanted rabbits that were studied with both modes of stimulation (Wilcoxon signed-rank test, $p = 0.08$). Moreover, a linear regression showed no effect of duration of deafness (the time interval between implantation and recording) on pulse-locking limits ($R^2 = 0.0002$, $p = 0.89$). Finally, pulse-locking limits were not correlated with spontaneous firing rates across the sample of neurons ($R^2 = 0.022$, $p = 0.15$).

Previous studies of the IC using anesthetized preparations (Snyder et al., 1995; Vollmer et al., 1999, 2005) have reported an inverse correlation between pulse-locking limit and spike latency in response to pulsatile CI stimulation. To assess whether such a correlation also holds in awake rabbit, the spike latency in response to pulse trains was calculated from the largest peak in the cross-correlogram (which excludes the onset response). Only responses to low-rate pulse trains (< 80 pps) were used to avoid ambiguities arising when the latency becomes comparable to the interpulse interval. The mode of the latency distribution was centered at 6–7 ms, with a minority of units (23%) having latencies >10 ms (Fig. 4*B*). In contrast to previous reports from anesthetized preparations, there was no significant correlation between pulse-locking limit and spike latency in awake rabbit ($R^2 = 0.006$, $p = 0.47$; Fig. 4*C*). This lack of correlation occurs because some long-latency units had a pulse-locked response up to relatively high rates. Previous studies in anesthetized animals measured the first-spike latency in response to the entire pulse train rather than the latency in response to each individual pulse in the train (excluding the onset response). To determine whether this difference in the definition of latency might account for the contrasting findings, we reanalyzed data from previous experiments in anesthetized cat (Hancock et al., 2010, 2012, 2013) using cross-correlation to determine latency and pulse-locking limits. There was a significant negative correlation between the two metrics ($R^2 = 0.36$, $p < 0.001$; Fig. 4*C*) in anesthetized cat, suggesting that the failure to observe such a correlation in awake rabbit reflects genuine differences between the two preparations rather than differences in the definition of latency.

Effect of barbiturate on spontaneous activity and response to pulse trains

The response properties of IC neurons in awake rabbit possess unique features that have not been reported in previous studies of responses to CI stimulation that used anesthetized preparations (Snyder et al., 1991, 1995; Vollmer et al., 1999, 2005; Hancock et al., 2010, 2012, 2013). These features include prominent spontaneous activity, a high incidence of suppressive responses to pulse trains, and unsynchronized, sustained responses at high pulse rates. To assess directly whether these differences reflect a specific effect of anesthesia as opposed to other methodological differ-

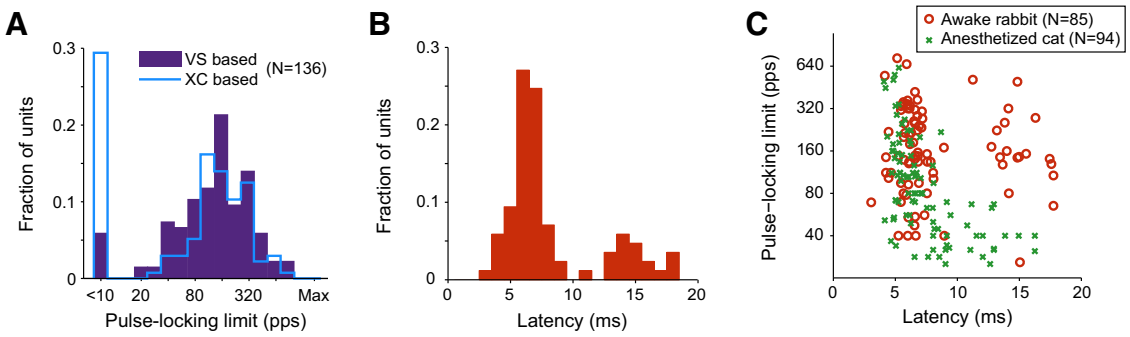

Figure 4. ***A***, Histogram of the distribution of pulse-locking limits based on cross-correlation and vector strength across the population of IC neurons in awake rabbit. ***B***, Distribution of spike latencies to low-rate pulse trains in awake rabbit. ***C***, Scatter plot of pulse-locking limit against spike latency in awake rabbit and anesthetized cat.

Table 1. Pulse-locking limits by method and preparation

	Cross-correlation			Vector strength			
Method	Unsync	Median (pps)[a]	IQR (pps)	Unsync	Median (pps)[a]	IQR (pps)	XC vs VS
Awake rabbit	29%	148	103–272	6%	158	80–274	$p = 0.13$[b]
Anesthetized cat	20%	80	45–150	8%	74	40–137	$p = 0.08$[b]
Rabbit vs cat	$p = 0.07$[c]	$p < 0.001$[d]		$p = 0.57$[c]	$p < 0.001$[d]		

[a]Pulse-locked units only.
[b]Kolmogorov–Smirnov test.
[c]χ^2 test.
[d]Wilcoxon rank-sum test.

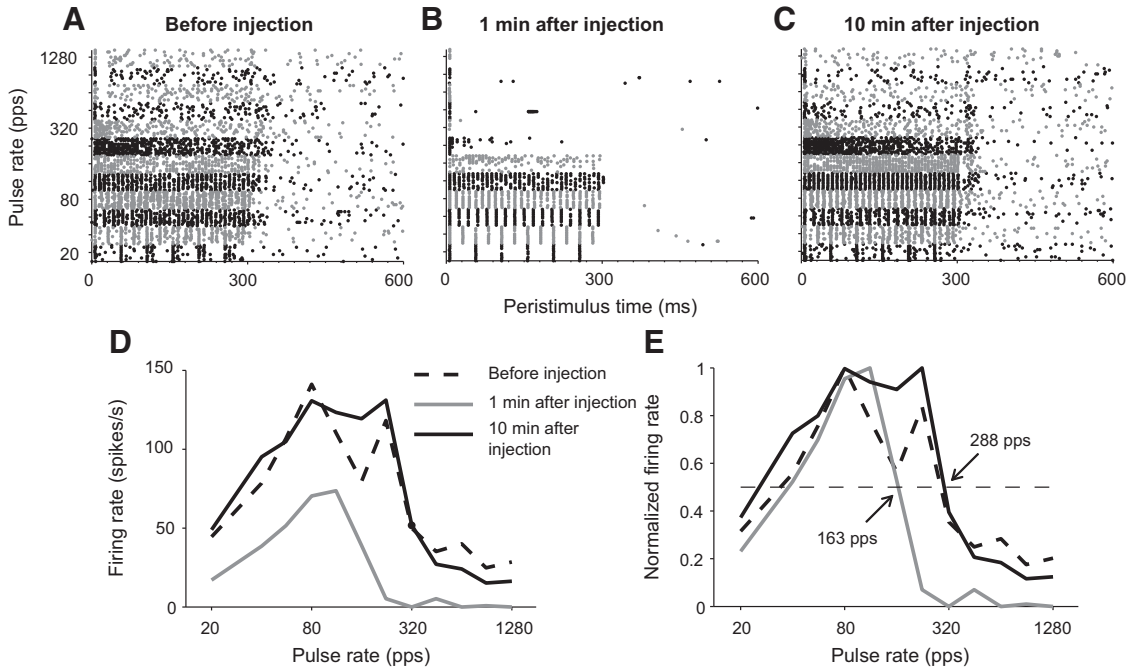

Figure 5. Effect of barbiturate on responses to pulse trains in a single unit from rabbit IC. ***A–C***, Temporal response patterns (dot rasters) just before injection (***A***), 1 min after injection (***B***), and 10 min after injection (***C***). ***D–E***, Absolute (***D***) and normalized (***E***) firing rate during the on period against pulse rate for the three time periods in ***A–C***.

ences with these earlier studies (none of which was conducted in rabbit), we monitored changes in the responses of 13 single units after intravenous injection of an ultra-short-acting barbiturate in one unilaterally implanted rabbit.

Illustrative results are presented in Figure 5 for one neuron. Before injection (Fig. 5*A*), the neuron showed background activity, clear pulse-locked spikes up to 320 pps, and unsynchronized sustained firing at higher pulse rates. One minute after injection (Fig. 5*B*), the background activity largely disappeared, pulse-locked responses were observed only up to 160 pps and there was no sustained activity at higher pulse rates. Ten minutes after injection (Fig. 5*C*), the response largely recovered back to the preinjection pattern. The firing rate was not uniformly attenuated across all pulse rates after injection, but rather the relative reduction was more pronounced at high pulse rates so that the "half-maximum pulse rate," where the firing rate falls to 50% of its maximum value, shifted to a lower value (Fig. 5*D*). This change in half-maximum rate is especially apparent when

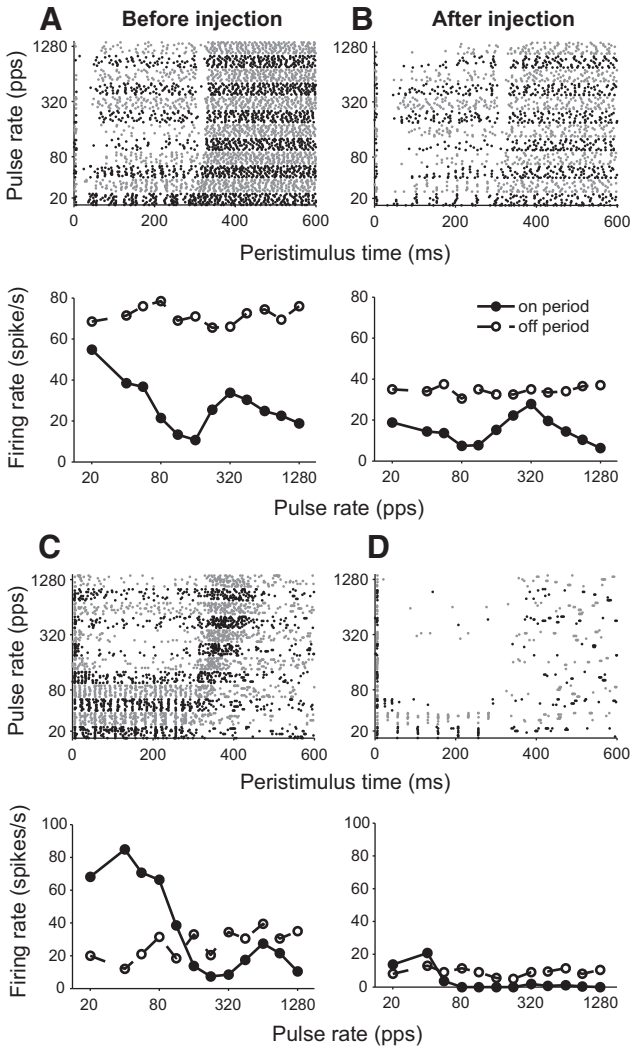

Figure 6. Effect of barbiturate in two single units from rabbit IC. ***A–B***, Unit with high spontaneous rate and suppressive responses to pulse trains. ***C–D***, Unit with multiple spike responses to each pulse at low rates and rebound responses at high pulse rates. For each unit and condition, temporal discharge patterns are shown on the top and mean firing rates during on and off periods versus pulse rate on the bottom.

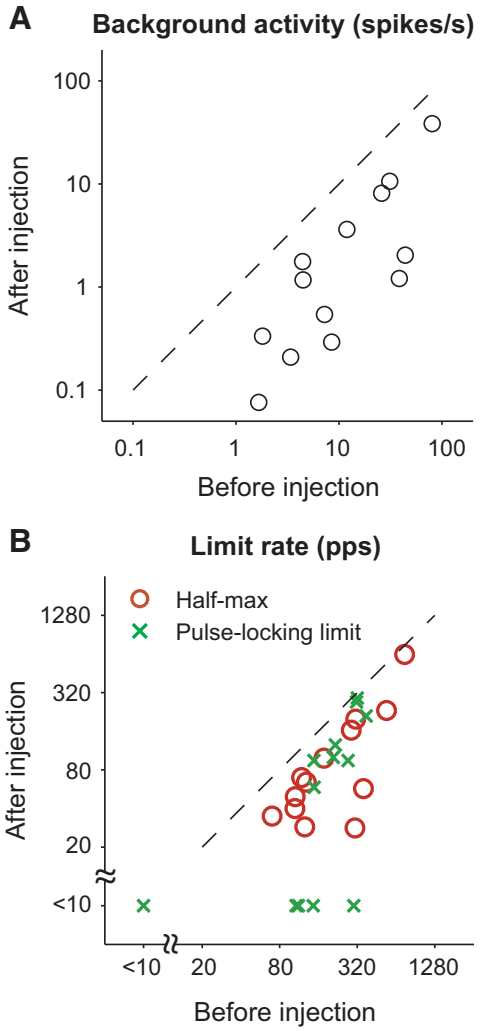

Figure 7. ***A***, Scatter plot of background firing rate before and 1–2 min after injection in the 13 units studied with barbiturate injections. ***B***, Scatter plots of half-maximum pulse rate and pulse-locking limit before and 1–2 min after injection.

the pre- and postinjection curves are each normalized by their maximum (Fig. 5*E*).

Two additional examples with different response patterns are presented in Figure 6. Before injection, the neuron in Figure 6, *A* and *B*, showed high background activity of ~70 spikes/s and firing was strongly suppressed during pulse train stimulation. One minute after injection, the background firing rate was reduced to half its preinjection value and the firing rate during the stimulus was also reduced, especially at low pulse rates. The unit in Figure 6, *C* and *D*, fired several spikes per pulse at low pulse rates before injection and showed pronounced rebound responses at high pulse rates. One minute after injection, the background activity was greatly reduced, pulse-locked responses were limited to 20 and 40 pps, and rebound responses were eliminated.

Three metrics were used to characterize these changes for the 13 single units studied with barbiturate injection: the background firing rate between stimulus presentations, the pulse-locking limit based on cross-correlograms, and the half-maximum pulse rate. Figure 7*A* compares the background firing rates before and after barbiturate injection across the unit sample. Background activity was decreased in all units and the median decrease in background rate (from 8.6 to 1.2 spikes/s) across the sample was statistically significant (Wilcoxon signed-rank test, $p < 0.001$). Figure 7*B* compares the preinjection and postinjection half-maximum rates and pulse-locking limits. All of the data points lie below the main diagonal, meaning that both the half-maximum rate and the pulse-locking limit were decreased after injection in all 13 units studied. In five units, pulse locking was completely eliminated. The median changes in half-maximum rate (from 176 to 64 pps) and pulse-locking limit (from 224 to 95 pps) across the unit sample were both highly significant (Wilcoxon signed-rank tests, $p < 0.001$ for both). However, the median response latencies measured by cross-correlation were not significantly altered by anesthesia (Wilcoxon signed-rank test, $p = 0.48$), which is consistent with the lack of correlation between latency and pulse-locking limit in the awake state (Fig. 4*C*).

Comparison with results from anesthetized cat

We have shown that injection of barbiturate anesthesia causes decreases in background activity, pulse-locking limits, and sustained responses to high rate stimulation in a small number of single units from rabbit IC. The response properties altered by anesthesia in rabbit are precisely those that distinguish results in

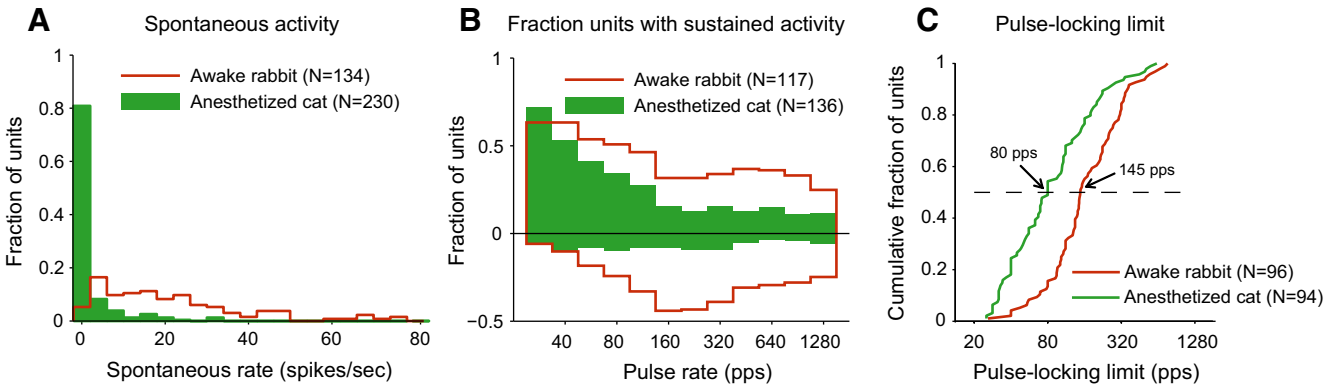

Figure 8. Comparison between response properties of sample IC neurons from awake rabbit and anesthetized cat. ***A***, Distribution of SRs. ***B***, Fraction of IC units showing sustained excitatory (positive ordinates) and suppressive (negative ordinates) responses to pulse-train stimulation as a function of pulse rate. ***C***, Cumulative distribution of pulse-locking limits using cross-correlation method excluding units that do not pulse lock at any rate.

the awake rabbit preparation from responses previously measured in anesthetized animals with CI stimulation, suggesting that anesthesia is a major factor underlying the differences with previous studies. However, the sample of units studied with barbiturate injection is too small ($n = 13$) to allow a detailed, quantitative comparison with these earlier studies at the neural population level. Moreover, the level of anesthesia induced by the ultra-short-acting barbiturate in rabbit is not as deep as the level used in previous studies (which were based on nonsurvival experiments), so that the effects of anesthesia are likely to be underestimated in the rabbit.

To address these issues, we reanalyzed data from previous experiments in anesthetized cats (Hancock et al., 2010, 2012, 2013) that used the same intracochlear electrodes, pulse train stimuli, and recording methods to quantitatively compare key response properties of IC neurons in the awake rabbit with those in an anesthetized preparation. This anesthetized cat preparation has been the leading animal model for studies of neural coding with CI stimulation in both the IC (Snyder et al., 1991, 1995; Vollmer et al., 1999, 2005; Shepherd et al., 2001; Smith and Delgutte, 2007; Middlebrooks and Snyder, 2010) and auditory cortex (Raggio and Schreiner, 1994, 1999, 2003; Kral et al., 2000, 2005, 2009; Fallon et al., 2009). Specifically, data from 117 single units in six bilaterally implanted, anesthetized cats were analyzed. Unless otherwise noted, data from both short-term-deafened (1 week) and long-term-deafened (6 months) cats were combined because the differences between the two groups were minor for the response measures of interest.

Spontaneous activity

There were obvious differences in spontaneous activity between anesthetized cats and awake rabbits. Figure 8*A* shows histograms of the distribution of spontaneous firing rates (SRs) across our neuron samples in the two preparations. Approximately 94% of units in awake rabbit had SRs > 1 spike/s with a median SR of 17.27 spikes/s. In contrast, a majority of units in anesthetized cats did not have any SRs and only 25% of the units had SRs >1 spike/s. The difference in SR distributions between the two preparations was highly significant (Kolmogorov–Smirnov test, $p < 0.001$).

We reported previously that spontaneous firing rates are higher in long-term-deafened cats than in short-term-deafened cats (Hancock et al., 2013), which might confound the comparison with the rabbit data when both groups of cats are combined. However, the median spontaneous rates in awake rabbit (17.27 spike/s) were significantly higher than those in long-term-deafened cats (0.10 spike/s; Wilcoxon rank-sum test, $p < 0.001$).

Prevalence of excitatory and suppressive responses

There were also major differences in the prevalence of excitatory and suppressive responses between the two preparations. In anesthetized cats, the fraction of units showing significant excitatory responses dropped rapidly with increasing pulse rate so that only 11–15% of the units had an excitatory response for rates of 160 pps and above (Fig. 8*B*). Although a drop with increasing pulse rates is also observed in awake rabbit, the fraction of units with excitatory responses remains >30% for all pulse rates and is higher is higher than the cat fraction for all pulse rates except 20 pps. A two-way ANOVA on the arc-sine-transformed data showed significant effects of both pulse rate and preparation ($p < 0.001$ for both). There is an even clearer contrast in suppressive response between the two preparations. Only 5–10% of the units at in anesthetized cat show a suppressive response for any pulse rate, as opposed to 20–50% in awake rabbits. A two-way ANOVA showed a significant effect of preparation on the incidence of suppressive responses ($p < 0.001$) but no effect of pulse rate ($p = 0.48$).

Temporal coding

Using the cross-correlation method to determine pulse locking, there were fewer neurons that did not pulse lock at any rate in anesthetized cat (20%) than in awake rabbit (28%) (Table 1). This result is consistent with the high incidence of suppressive responses that did not give rise to a short-latency cross-correlogram peak in rabbit. Among the units that did show pulse locking, the distribution of pulse-locking limits based was strongly biased toward higher rates in awake rabbit compared with anesthetized cat and this held for both the cross-correlation method and the vector strength method. The difference is clearly apparent in the cumulative distributions based on the cross-correlation method (Fig. 8*C*), which include only pulse-locking units. The median pulse-locking limit was 1.9 times higher in awake rabbit (148 pps) than in anesthetized cat (80 pps). Approximately 50% of pulse-locking limits fell in the range 45–150 pps in anesthetized cat versus 103–272 pps in awake rabbit. The difference in median pulse-locking limits between the two preparations was highly significant when only pulse-locking units were compared (Wilcoxon rank sum test, $p < 0.001$) and remained significant ($p = 0.03$) when all units were included despite the higher proportion of unsynchronized units in rabbit.

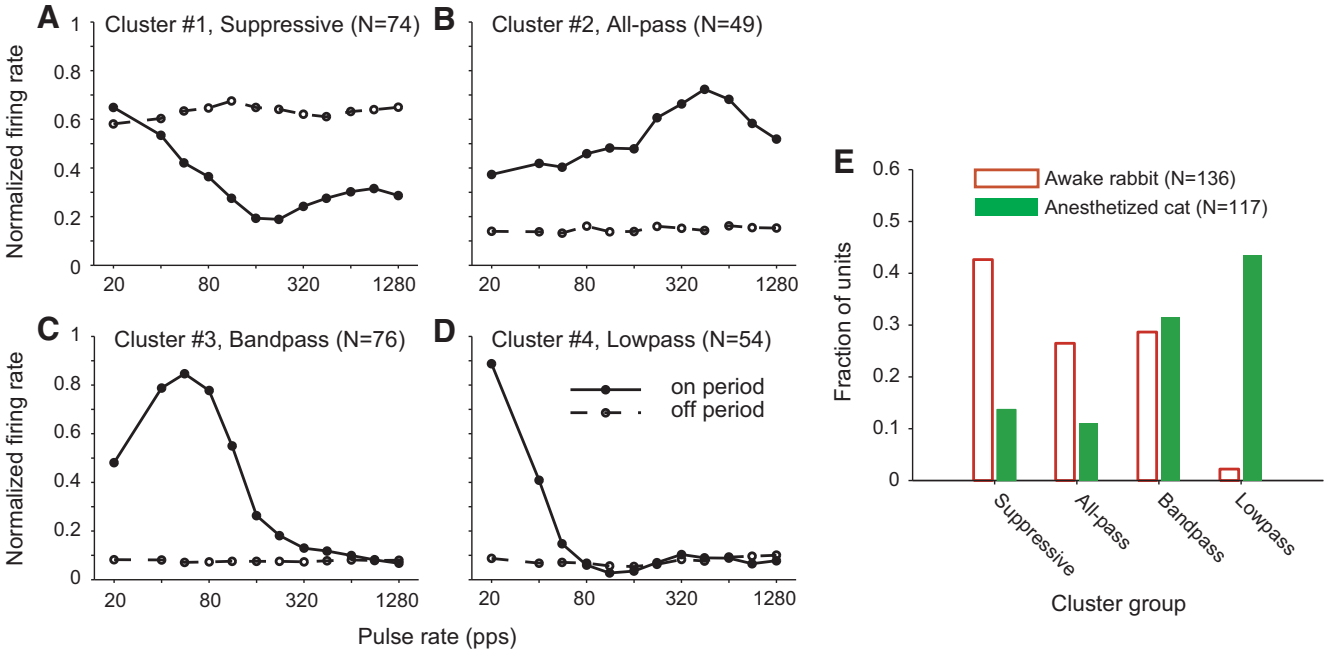

Figure 9. Neurons clusters based on on period and off period responses to pulse train stimuli. ***A–D***, Centroids of the four neuron clusters generated by *k*-means clustering. Each curve shows the normalized mean firing rate during the on and off periods as a function of pulse rate. ***A***, "Suppressive" cluster. ***B***, "All-pass" cluster. ***C***, "Band-pass" cluster. ***D***, "Low-pass" cluster. ***E***, Relative incidence of each cluster differs between the two preparations.

In summary, the three effects that were observed directly in a few rabbit single units after barbiturate injection (i.e., decreases in background activity, pulse-locking limits, and incidence of excitatory responses at high pulse rates) are also observed when response properties are compared quantitatively across much larger samples of IC neurons from awake rabbit and anesthetized cat, suggesting that anesthesia is a major factor underlying the differences between the two preparations.

Characterization of the variability in pulse rate dependence of on and off responses

The example neurons in Figures 1 illustrate the wide variability that was observed in both the pulse-rate dependence of responses to pulse trains and the degree to which responses are primarily excitatory or suppressive. To characterize this variability objectively, we used *k*-means clustering to categorize the various response patterns observed in awake rabbit and anesthetized cat (see Materials and Methods). This clustering analysis was applied to the combined data from both preparations so that the full range of variability would be represented and the distributions of the different clusters could be compared between the two preparations. We chose to split the neuron population into four clusters because this categorization accounted for >50% of the variance in the data and the clusters were easily interpretable. The pulse rate dependence of responses for the four cluster centroids is shown in Figure 9, *A–D*. The first cluster (Fig. 9*A*) contains neurons with predominantly suppressive responses, in that the off period response is greater than the on period response at most pulse rates. The other three clusters (Fig. 9*B–D*) contain predominantly excitatory responses but differ in the pulse rate yielding the largest response. Cluster 2 (Fig. 9*B*) contains "all-pass" neurons that have an excitatory response over a broad range of pulse rates, often with the maximum firing rate occurring at higher pulse rates (> 320 pps). Cluster 3 (Fig. 9*C*) contains "band-pass" neurons that have a maximum in firing rate near 80 pps, with a clear drop on either side. Finally, Cluster 4 (Fig. 9*D*) contains "low-pass" neurons in which the firing rate decreases rapidly with increasing pulse rate and there is little or no sustained response >80 pps. The example neurons in Figure 1, *A–D*, belong to the suppressive, all-pass, band-pass, and low-pass clusters, respectively.

The relative incidence of the four response types differed markedly between the two preparations (χ^2 test, $p < 0.001$; Fig. 9*E*). In awake rabbit, the most common response pattern was the suppressive type (43%), followed by band-pass and all-pass responses in similar proportions (25–30%). Very few neurons in awake rabbit showed the low-pass response pattern. In contrast, the most common response pattern in anesthetized cats was low-pass followed by band-pass. <14% of units in anesthetized cats showed all-pass or suppressive responses. There was no significant difference in the distribution of neurons across the four clusters between unilaterally deafened rabbits and bilaterally deafened rabbits (χ^2 test, $p = 0.92$).

The four clusters defined based on average firing rates also differ in pulse-locked responses. Figure 10 shows both the pulse-locked firing rate (as presented in Fig. 3*G*,*H*) and the overall firing rate as a function of pulse rate for each of the four cluster centroids defined in Figure 9. In suppressive neurons (Fig. 10*A*), the pulse-locked firing rate is much lower than the overall firing rate for all pulse rates, reflecting the lack of a sharp peak in the cross-correlogram for these neurons, which are mostly recorded from awake rabbit. All-pass neurons (Fig. 10*B*) show a similar dependence of overall and pulse-locked firing rates at low pulse rates, but the pulse-locked rate begins to fall markedly for pulse rates >224 pps. At high pulse rates (>320 pps), the overall firing rate is much larger than the pulse-locked rate, which is characteristic of the sustained, unsynchronized responses only observed significantly in awake rabbit. In band-pass neurons (Fig. 10*C*), the pulse-locked firing rate approximately parallels the overall firing rate with some attenuation. Finally, in low-pass

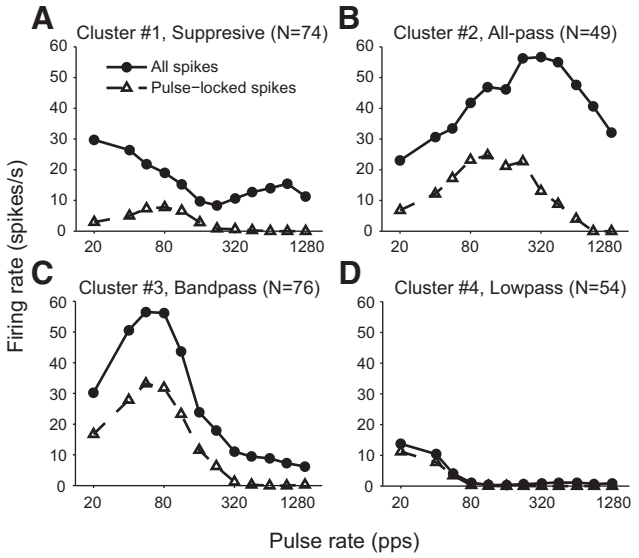

Figure 10. Mean pulse-locked firing rate and overall firing rate as a function of pulse rate for each of the four neuron clusters defined from rate responses to pulse trains. ***A–D***, Same as in Figure 9.

neurons (Fig. 10*D*), there is little difference between pulse-locked and overall firing rates, consistent with the lack of background activity in these neurons, which overwhelmingly come from anesthetized cats.

Discussion

We measured the responses of single units in IC of awake rabbit to electric pulse trains delivered through intracochlear electrode arrays. Compared with results from anesthetized preparations, IC neurons in rabbit showed higher spontaneous activity and greater sustained responses (excitatory or suppressive) to high-rate pulse trains. Temporal coding of pulse trains was also enhanced at high pulse rates. Decreases in background activity, pulse-locking limits, and sustained responses at pulse high rates were observed directly in a small number of single units from one rabbit after injection of an ultra-short-acting barbiturate. These changes were consistent with quantitative differences between much larger samples of neurons between the awake rabbit preparation and earlier data from anesthetized cats, suggesting that anesthesia is a major factor underlying these differences. Nevertheless, other methodological differences between the two preparations with respect to species, recording electrodes, timing of deafness, and auditory experience with cochlear implants could also contribute to the observed effects.

The majority of the data came from two unilaterally implanted rabbits that had hearing in the unimplanted ear. In this respect, these rabbits differed from most human cochlear implant users, who are usually profoundly deaf on both sides. Unilateral deafening in adult animals has been shown to cause increased responsiveness to acoustic stimulation of the intact ear in the ipsilateral IC, an effect attributed to downregulation of inhibition (Popelár et al., 1994; McAlpine et al., 1997; Mossop et al., 2000; Vale et al., 2004). Although similar changes are likely to have occurred in the unilaterally implanted rabbits, possibly also altering the responses to electric stimulation of the contralateral ear, we observed no difference in spontaneous activity, incidence of excitatory responses to pulse trains, and upper limit of pulse locking between monaural stimulation of the contralateral ear in unilaterally implanted rabbits and diotic stimulation in bilaterally implanted rabbits, which were profoundly deaf on both sides. However, the power of these statistical tests was limited by the relatively small number of units (42) sampled in the bilaterally implanted rabbits.

Increased spontaneous activity and suppressive responses in IC of awake rabbit

We found a much higher level of spontaneous activity in awake rabbits compared with anesthetized cats. The background activity occurring between stimulus presentations in individual neurons was decreased by injection of barbiturate in one rabbit. Studies in normal-hearing animals have generally reported that barbiturate anesthesia decreases spontaneous activity in both the IC (Bock and Webster, 1974; Kuwada et al., 1989; Torterolo et al., 2002) and the auditory cortex (Zurita et al., 1994), although one study found no effect (Ter-Mikaelian et al., 2007). Other studies show that hearing loss produced by either exposure to loud sounds (Basta and Ernest, 2004; Wang et al., 2011; Manzoor et al., 2012; Robertson et al., 2013) or ototoxic drugs (Shepherd and Javel, 1999; Hancock et al., 2010, 2013) also results in increased spontaneous activity in the tonotopic region of hearing loss in the IC and other auditory nuclei. All of these studies were conducted in anesthetized animals. Whether the effects of hearing loss on spontaneous activity are amplified in the awake state is an important question for a mechanistic understanding of the tinnitus frequently associated with hearing loss.

The unmasking of spontaneous activity in the awake state revealed suppressive responses to electric stimulation that were observed frequently in the rabbit, but are rarely observed in anesthetized animals. Suppression of spontaneous activity may be a neural substrate for the suppression of tinnitus by electric stimulation reported in some CI users (Rubinstein et al., 2003; Van de Heyning et al., 2008; Chang and Zeng, 2012).

Mechanisms of anesthesia effects

Higher evoked firing rates in awake animals have been observed in the IC of normal-hearing rabbits (Kuwada et al., 1989) and guinea pigs (Torterolo et al., 2002) and in the primary auditory cortex of deaf marmosets and guinea pigs with CI stimulation (Johnson et al., 2011; Kirby and Middlebrooks, 2012). Using "precedence effect" stimuli, Tollin et al. (2004) found shorter suppression of the response to the lagging click by the leading click in the IC of awake, behaving cat compared with barbiturate-anesthetized cat (Litovsky and Yin, 1998). A similar effect of barbiturates on recovery times has also been observed in rat IC (Song et al., 2011). Shorter suppression may lead to improved temporal coding of acoustic stimuli at high stimulation rates, which is consistent with our finding of higher pulse-locking limits in awake rabbit.

The reduction in spontaneous and evoked firing rates and the prolongation of recovery times by anesthesia are consistent with an enhancement of inhibition mediated by GABA receptors, as suggested by Kuwada et al. (1989). However, in auditory thalamic neurons, the suppressive effect of pentobarbital on evoked firing rates was not eliminated by iontophoresis of GABA receptor antagonists, suggesting that additional mechanisms are involved (Wan and Puil, 2002). The urethane anesthesia used in our cat preparation acts via a wide spectrum of neurotransmitter-gated ion channels (Hara and Harris, 2002), so the effects of anesthesia are likely to be even more complex.

Earlier reports (Colburn et al., 2009; Hancock et al., 2012) suggested that the upper rate limit on pulse-locked responses to electric pulse trains may be mediated by the low-threshold, voltage activated potassium currents ($I_{K,LVA}$) present in many brain-

stem auditory neurons, including medial superior olivary neurons (Svirskis et al., 2004). Neurons expressing $I_{K,LVA}$ show a cumulative increase in membrane conductance after each stimulus pulse that increases the spiking threshold (Manis and Marx, 1991). Barbiturates decrease excitatory neurotransmitter release by reducing voltage-dependent calcium conductances (Werz and Macdonald, 1985). The resulting reduction of excitatory drive may further limit the ability of neurons to reach threshold at high pulse rates under anesthesia.

Perceptual implications of higher coding of high-rate pulse trains

The temporal coding of constant-amplitude pulse trains by IC neurons has been studied extensively in anesthetized preparations, with a focus on characterizing the maximum pulse rate for which responses are synchronized ("pulse-locked") to the stimulus (Snyder et al., 1995; Vollmer et al., 1999, 2005; Middlebrooks and Snyder, 2010). Using the Rayleigh test for vector strength as a pulse-locking criterion, median pulse-locking limits of IC neurons for intracochlear stimulation range from 95 pps (Vollmer et al., 2005) to 120 pps (Middlebrooks and Snyder, 2010). (Higher limits were obtained with intraneural stimulation of the auditory nerve, which facilitates the stimulation of low-frequency tonotopic regions.) Despite differences among these studies in timing of deafness, stimulation regimens, pulse-locking criteria, and unit selection criteria, temporal coding limits in awake rabbit (median 158 pps using the vector strength method) are clearly higher than those from these anesthetized preparations.

Our finding of higher pulse-locking limits in awake rabbit contrasts with those of Ter-Mikaelian et al. (2007), who observed no difference in the phase- locking limits of IC neurons to sinusoidally amplitude modulated (SAM) tones between anesthetized and unanesthetized gerbils, even though these investigators found clear effects of anesthesia in the auditory cortex. A transition from sustained to onset response was clearly observed at high pulse rates for individual neurons in a unilaterally deaf rabbit after administration of barbiturate (Fig. 7*A–C*). Such transitions may be less common in normal-hearing animals, in which both SAM tones and pulse trains can already produce sustained responses at high rates even under anesthetized conditions (Krishna and Semple, 2000; Nelson and Carney, 2007; Krebs et al., 2008).

The higher temporal coding limits of IC neurons in awake rabbits better agree with human performance in temporal processing tasks such as rate pitch discrimination. Most CI listeners can discriminate the rate of periodic pulse trains and rank them based on perceived pitch up to ~300 pps (Moore and Carlyon, 2010). A few "star subjects" show an ability to detect changes in pulse rate perhaps as high as 1000 pps (Townshend et al., 1987; Kong et al., 2009; Kong and Carlyon, 2010). Temporal coding in awake rabbit, where >20% of the neurons had temporal pulse-locking limits ≥224 pps, seems sufficient to account for the rate discrimination abilities of the "typical" CI user. However, the performance of the star subjects still seems hard to account for from the awake IC data.

Pulse rates >300 pps might be coded by the firing rates of IC neurons giving unsynchronized, sustained responses to high-rate pulse trains, which were common in awake rabbit. Such sustained, unsynchronized responses are rarely observed in anesthetized animals. Unsynchronized activity to high-rate stimulation was first described in the primary auditory cortex (Lu et al., 2001; Wang et al., 2008) and thalamus (Bartlett and Wang, 2007) of normal-hearing, awake marmosets, but were rarely observed in the auditory cortex of anesthetized cats (Lu and Wang, 2000). Subsequently, unsynchronized activity to electric stimulation through CI was also observed in the primary auditory cortex of awake, deaf animals (Johnson et al., 2011; Kirby and Middlebrooks, 2012). The crossover pulse rate where unsynchronized responses become more prevalent than pulse-locked responses was 224 pps in deaf rabbits (data not shown), which is much higher than the ~50 pps crossover rate in the auditory cortex of normal-hearing marmosets (Liu et al., 2001; Fig. 3) and still higher than the ~120 pps crossover in marmoset thalamus (Bartlett and Wang, 2007; Fig. 3). The presence of sustained responses at high pulse rates in the IC and cortex of awake animals is consistent with auditory percepts lasting throughout the stimulus duration in most CI users (Tang et al., 2006).

In the IC of anesthetized animals, sensitivity to ITDs for periodic electric pulse trains is reduced or eliminated at high pulse rates (Smith and Delgutte, 2007; Hancock et al., 2012). Perceptual sensitivity to ITDs also degrades at high stimulation rates in bilateral CI users (Laback et al., 2007; van Hoesel, 2007), but the perceptual limits (250–600 pps) are higher than the limits for most IC neurons in anesthetized cat. It has been suggested that the limits on rate discrimination and ITD sensitivity with CI stimulation may share a common mechanism (van Hoesel, 2007; Carlyon et al., 2008). Whether the enhanced pulse locking at high rates in awake rabbits also translates to improved ITD sensitivity in bilaterally implanted animals will be of interest in future studies and will shed light on the nature of the perceptual limitations.

References

Bartlett EL, Wang X (2007) Neural representations of temporally modulated signals in the auditory thalamus of awake primates. J Neurophysiol 97:1005–1017. CrossRef Medline

Basta D, Ernest A (2004) Noise-induced changes of neuronal spontaneous activity in mice inferior colliculus brain slices. Neurosci Lett 368:297–302. CrossRef Medline

Bock GR, Webster WR (1974) Spontaneous activity of single units in the inferior colliculus of anesthetized and unanesthetized cats. Brain Res 76:150–154. CrossRef Medline

Carlyon RP, Long CJ, Deeks JM (2008) Pulse-rate discrimination by cochlear-implant and normal-hearing listeners with and without binaural cues. J Acoust Soc Am 123:2276–2286. CrossRef Medline

Chang JE, Zeng FG (2012) Tinnitus suppression by electric stimulation of the auditory nerve. Front Syst Neurosci 6:19. CrossRef Medline

Chung Y, Hancock KE, Nam SI, Delgutte B (2013) Better temporal neural coding with cochlear implants in awake animals. Adv Exp Med Biol 787:353–361. CrossRef Medline

Colburn HS, Chung Y, Zhou Y, Brughera A (2009) Models of brainstem responses to bilateral electrical stimulation. J Assoc Res Otolaryngol 10:91–110. CrossRef Medline

Day ML, Koka K, Delgutte B (2012) Neural encoding of sound source location in the presence of a concurrent, spatially separated source. J Neurophysiol 108:2612–2628. CrossRef Medline

Devore S, Delgutte B (2010) Effects of reverberation on the directional sensitivity of auditory neurons across the tonotopic axis: influences of interaural time and level differences. J Neurosci 30:7826–7837. CrossRef Medline

Ebert CS, Fitzpatrick DC, Cullen RD, Finley CC, Bassim MK, Zdanski CJ, Coffey CS, Crocker W, Skaggs J, Marshall AF, Falk SE (2004) Responses of binaural neurons to combined auditory and electrical stimulation. Assoc Res Otolaryngol Abstr 27:485.

Fallon JB, Irvine DR, Shepherd RK (2009) Cochlear implant use following neonatal deafness influences the cochleotopic organization of the primary auditory cortex in cats. J Comp Neurol 512:101–114. CrossRef Medline

Goldberg JM, Brown PB (1969) Response of binaural neurons of dog superior olivary complex to dichotic tonal stimuli: some physiological mechanisms of sound localization. J Neurophysiol 32:613–636. Medline

Hancock KE, Noel V, Ryugo DK, Delgutte B (2010) Neural coding of inter-

aural time differences with bilateral cochlear implants: effects of congenital deafness. J Neurosci 30:14068–14079. CrossRef Medline

Hancock KE, Chung Y, Delgutte B (2012) Neural ITD coding with bilateral cochlear implants: effect of binaurally coherent jitter. J Neurophysiol 108: 714–728. CrossRef Medline

Hancock KE, Chung Y, Delgutte B (2013) Congenital and prolonged adult-onset deafness cause distinct degradations in neural ITD coding with bilateral cochlear implants. J Assoc Res Otolaryngol 14:393–411. CrossRef Medline

Hara K, Harris RA (2002) The anesthetic mechanism of urethane: the effects on neurotransmitter-gated ion channels. Anesth Analg 94:313–318, table of contents. Medline

Johnson L, Santina CD, Wang X (2011) Neural responses to cochlear implant stimulation in auditory cortex of awake marmeset. Assoc Res Otolaryngol Abstr 34:943.

Kaplan HM, Timmons EH (1979) advanced specialized procedures. In: The rabbit: a model for the principles of mammalian physiology and surgery (Kaplan HM, ed). San Diego: Academic.

Kirby AE, Middlebrooks JC (2012) Unanesthetized auditory cortex exhibits multiple codes for gaps in cochlear implant pulse trains. J Assoc Res Otolaryngol 13:67–80. CrossRef Medline

Kong YY, Carlyon RP (2010) Temporal pitch perception at high rates in cochlear implants. J Acoust Soc Am 127:3114–3123. CrossRef Medline

Kong YY, Deeks JM, Axon PR, Carlyon RP (2009) Limits of temporal pitch in cochlear implants. J Acoust Soc Am 125:1649–1657. CrossRef Medline

Kral A, Hartmann R, Tillein J, Heid S, Klinke R (2000) Congenital auditory deprivation reduces synaptic activity within the auditory cortex in a layer-specific manner. Cereb Cortex 10:714–726. CrossRef Medline

Kral A, Tillein J, Heid S, Hartmann R, Klinke R (2005) Postnatal cortical development in congenital auditory deprivation. Cereb Cortex 15:552–562. CrossRef Medline

Kral A, Tillein J, Hubka P, Schiemann D, Heid S, Hartmann R, Engel AK (2009) Spatiotemporal patterns of cortical activity with bilateral cochlear implants in congenital deafness. J Neurosci 29:811–827. CrossRef Medline

Krebs B, Lesica NA, Grothe B (2008) The representation of amplitude modulations in the mammalian auditory midbrain. J Neurophysiol 100:1602–1609. CrossRef Medline

Krishna BS, Semple MN (2000) Auditory temporal processing: responses to sinusoidally amplitude-modulated tones in the inferior colliculus. J Neurophysiol 84:255–273. Medline

Kuwada S, Batra R, Stanford TR (1989) Monaural and binaural response properties of neurons in the inferior colliculus of the rabbit: effects of sodium pentobarbital. J Neurophysiol 61:269–282. Medline

Laback B, Majdak P, Baumgartner WD (2007) Lateralization discrimination of interaural time delays in four-pulse sequences in electric and acoustic hearing. J Acoust Soc Am 121:2182–2191. CrossRef Medline

Litovsky RY, Yin TC (1998) Physiological studies of the precedence effect in the inferior colliculus of the cat. II. Neural mechanisms. J Neurophysiol 80:1302–1316. Medline

Litvak L, Delgutte B, Eddington D (2001) Auditory nerve fiber responses to electric stimulation: modulated and unmodulated pulse trains. J Acoust Soc Am 110:368–379. CrossRef Medline

Liu S, Aghakhani N, Boisset N, Said G, Tadie M (2001) Innervation of the caudal denervated ventral roots and their target muscles by the rostral spinal motoneurons after implanting a nerve autograft in spinal cord-injured adult marmosets. J Neurosurg 94:82–90. Medline

Lu T, Wang X (2000) Temporal discharge patterns evoked by rapid sequences of wide- and narrowband clicks in the primary auditory cortex of cat. J Neurophysiol 84:236–246. Medline

Lu T, Liang L, Wang X (2001) Temporal and rate representations of time-varying signals in the auditory cortex of awake primates. Nat Neurosci 4:1131–1138. CrossRef Medline

Manis PB, Marx SO (1991) Outward currents in isolated ventral cochlear nucleus neurons. J Neurosci 11:2865–2880. Medline

Manzoor NF, Licari FG, Klapchar M, Elkin RL, Gao Y, Chen G, Kaltenbach JA (2012) Noise-induced hyperactivity in the inferior colliculus: its relationship with hyperactivity in the dorsal cochlear nucleus. J Neurophysiol 108:976–988. CrossRef Medline

McAlpine D, Martin RL, Mossop JE, Moore DR (1997) Response properties of neurons in the inferior colliculus of the monaurally deafened ferret to acoustic stimulation of the intact ear. J Neurophysiol 78:767–779. Medline

Middlebrooks JC, Snyder RL (2010) Selective electrical stimulation of the auditory nerve activates a pathway specialized for high temporal acuity. J Neurosci 30:1937–1946. CrossRef Medline

Moore BCJ, Carlyon RP (2010) perception of pitch by people with cochlear hearing loss and by cochlear implant users. In: Pitch: neural coding and perception (Plack CJ, Oxenham AJ, Fay RR, eds), pp 234–277. New York: Springer.

Mossop JE, Wilson MJ, Caspary DM, Moore DR (2000) Down-regulation of inhibition following unilateral deafening. Hear Res 147:183–187. CrossRef Medline

Nelson PC, Carney LH (2007) Neural rate and timing cues for detection and discrimination of amplitude-modulated tones in the awake rabbit inferior colliculus. J Neurophysiol 97:522–539. CrossRef Medline

Popelár J, Erre JP, Aran JM, Cazals Y (1994) Plastic changes in ipsi-contralateral differences of auditory cortex and inferior colliculus evoked potentials after injury to one ear in the adult guinea pig. Hear Res 72:125–134. CrossRef Medline

Raggio MW, Schreiner CE (1994) Neuronal responses in cat primary auditory cortex to electrical cochlear stimulation. I. Intensity dependence of firing rate and response latency. J Neurophysiol 72:2334–2359. Medline

Raggio MW, Schreiner CE (1999) Neuronal responses in cat primary auditory cortex to electrical cochlear stimulation. III. Activation patterns in short- and long-term deafness. J Neurophysiol 82:3506–3526. Medline

Raggio MW, Schreiner CE (2003) Neuronal responses in cat primary auditory cortex to electrical cochlear stimulation: IV. Activation pattern for sinusoidal stimulation. J Neurophysiol 89:3190–3204. CrossRef Medline

Robertson D, Bester C, Vogler D, Mulders WH (2013) Spontaneous hyperactivity in the auditory midbrain: relationship to afferent input. Hear Res 295:124–129. CrossRef Medline

Rubinstein JT, Tyler RS, Johnson A, Brown CJ (2003) Electrical suppression of tinnitus with high-rate pulse trains. Otol Neurotol 24:478–485. CrossRef Medline

Shepherd RK, Javel E (1999) Electrical stimulation of the auditory nerve: II. Effect of stimulus waveshape on single fibre response properties. Hear Res 130:171–188. CrossRef Medline

Shepherd RK, Hardie NA, Baxi JH (2001) Electrical stimulation of the auditory nerve: single neuron strength-duration functions in deafened animals. Ann Biomed Eng 29:195–201. CrossRef Medline

Smith ZM, Delgutte B (2007) Sensitivity to interaural time differences in the inferior colliculus with bilateral cochlear implants. J Neurosci 27:6740–6750. CrossRef Medline

Snyder RL, Rebscher SJ, Leake PA, Kelly K, Cao K (1991) Chronic intracochlear electrical stimulation in the neonatally deafened cat. II. Temporal properties of neurons in the inferior colliculus. Hear Res 56:246–264. CrossRef Medline

Snyder R, Leake P, Rebscher S, Beitel R (1995) Temporal resolution of neurons in cat inferior colliculus to intracochlear electrical stimulation: effects of neonatal deafening and chronic stimulation. J Neurophysiol 73: 449–467. Medline

Song P, Wang N, Wang H, Xie Y, Jia J, Li H (2011) Pentobarbital anesthesia alters neural responses in the precedence effect. Neurosci Lett 498:72–77. CrossRef Medline

Svirskis G, Kotak V, Sanes DH, Rinzel J (2004) Sodium along with low-threshold potassium currents enhance coincidence detection of subthreshold noisy signals in MSO neurons. J Neurophysiol 91:2465–2473. CrossRef Medline

Tang Q, Liu S, Zeng FG (2006) Loudness adaptation in acoustic and electric hearing. J Assoc Res Otolaryngol 7:59–70. CrossRef Medline

Ter-Mikaelian M, Sanes DH, Semple MN (2007) Transformation of temporal properties between auditory midbrain and cortex in the awake Mongolian gerbil. J Neurosci 27:6091–6102. CrossRef Medline

Tollin DJ, Populin LC, Yin TC (2004) Neural correlates of the precedence effect in the inferior colliculus of behaving cats. J Neurophysiol 92:3286–3297. CrossRef Medline

Torterolo P, Falconi A, Morales-Cobas G, Velluti RA (2002) Inferior colliculus unitary activity in wakefulness, sleep and under barbiturates. Brain Res 935:9–15. CrossRef Medline

Townshend B, Cotter N, Van Compernolle D, White RL (1987) Pitch perception by cochlear implant subjects. J Acoust Soc Am 82:106–115. CrossRef Medline

Vale C, Juíz JM, Moore DR, Sanes DH (2004) Unilateral cochlear ablation produces greater loss of inhibition in the contralateral inferior colliculus. Eur J Neurosci 20:2133–2140. CrossRef Medline

Van de Heyning P, Vermeire K, Diebl M, Nopp P, Anderson I, De Ridder D (2008) Incapacitating unilateral tinnitus in single-sided deafness treated by cochlear implantation. Ann Otol Rhinol Laryngol 117:645–652. Medline

van Hoesel RJ (2007) Sensitivity to binaural timing in bilateral cochlear implant users. J Acoust Soc Am 121:2192–2206. CrossRef Medline

Vollmer M, Snyder RL, Leake PA, Beitel RE, Moore CM, Rebscher SJ (1999) Temporal properties of chronic cochlear electrical stimulation determine temporal resolution of neurons in cat inferior colliculus. J Neurophysiol 82:2883–2902. Medline

Vollmer M, Leake PA, Beitel RE, Rebscher SJ, Snyder RL (2005) Degradation of temporal resolution in the auditory midbrain after prolonged deafness is reversed by electrical stimulation of the cochlea. J Neurophysiol 93:3339–3355. CrossRef Medline

Wan X, Puil E (2002) Pentobarbital depressant effects are independent of GABA receptors in auditory thalamic neurons. J Neurophysiol 88:3067–3077. CrossRef Medline

Wang H, Brozoski TJ, Caspary DM (2011) Inhibitory neurotransmission in animal models of tinnitus: maladaptive plasticity. Hear Res 279:111–117. CrossRef Medline

Wang X, Lu T, Bendor D, Bartlett E (2008) Neural coding of temporal information in auditory thalamus and cortex. Neuroscience 154:294–303. CrossRef Medline

Werz MA, Macdonald RL (1985) Barbiturates decrease voltage-dependent calcium conductance of mouse neurons in dissociated cell culture. Mol Pharmacol 28:269–277. Medline

Xu SA, Shepherd RK, Chen Y, Clark GM (1993) Profound hearing loss in the cat following the single co-administration of kanamycin and ethacrynic acid. Hear Res 70:205–215. Medline

Yin TC, Kuwada S (1983) Binaural interaction in low-frequency neurons in inferior colliculus of the cat. III. Effects of changing frequency. J Neurophysiol 50:1020–1042. Medline

Zurita P, Villa AE, de Ribaupierre Y, de Ribaupierre F, Rouiller EM (1994) Changes of single unit activity in the cat's auditory thalamus and cortex associated to different anesthetic conditions. Neurosci Res 19:303–316. CrossRef Medline